King's Research Portal

Document Version
Publisher's PDF, also known as Version of record

Link to publication record in King's Research Portal

Transient gas and particle emissions from smouldering combustion of peat

Yuqi Hu, Eirik Christensen, Francesco Restuccia, Guillermo Rein*

Department of Mechanical Engineering, City and Guilds Building, Imperial College London, SW7 2AZ, UK

Abstract

Smouldering combustion of peat drives the largest fires on Earth, and their emissions play an important role in global carbon balance and regional air quality. Here we report a series of controlled laboratory experiments of peat fires. Peat samples of 100% moisture content in dry basis were burnt in an open-top reactor with dimensions of $20 \times 20 \times 10$ cm. The diagnostics are a unique set of simultaneous measurements consisting of real-time mass loss, up to 20 different gas species concentration, size-fractioned particle mass (PM_{10}, $PM_{2.5}$ and PM_1), temperature profile, and visual and infrared imaging. This comprehensive framework of measurements reveals that the evolution of the emissions varies in time with four observed stages (ignition, growth, steady and burn out) which are characterised by different combustion dynamics. Mass flux measurements show that CO_2, CO, CH_4 and NH_3 are the four most predominant gas species emitted in the steady stage. Incorporating the mass loss rate, the transient emission factors (EF_m) of both gas and particle species are calculated and reported here for the first time. Averaging the steady stage, the EFm of $PM_{2.5}$ reached 23.12 g kg^{-1}, which accounts for 87.2% of the total particle mass, and PM_1 EF_m was reported to be 15.04 g kg^{-1}. The EFm of alkane species (CH_4, C_2H_6, C_3H_8, C_4H_{10}) were found to peak within the ignition stage, whereas the EF_m of CO_2, CO and NH_3 kept increasing during the steady stage. Because of these measurements, for the first time we were able to validate the EF calculated by assuming averaged values and a carbon balance, which is the preferred method used in remote sensing and atmospheric sciences. This work contributes to a better understanding of peat fire emissions and could help develop strategies tackling regional haze.
© 2018 The Author(s). Published by Elsevier Inc. on behalf of The Combustion Institute.
This is an open access article under the CC BY license. (http://creativecommons.org/licenses/by/4.0/)

1. Introduction

Peat is a carbon-rich organic soil which is mainly made of partially decomposed plants, accumulated in water-logged and anaerobic conditions during centuries to millennia [1]. Unlike flaming forest fires, peat fires are dominated by smouldering combustion, the slow ($\sim$1 mm min^{-1} spread rate), low-temperature (peak $\sim$550–650°C), flameless burning of porous fuels, and the most persistent combustion phenomena [2,3]. In flaming combustion, homogeneous oxidation of the

Nomenclature

EF	emission factor (mass of species per mass of dry fuel burnt)
FTIR	Fourier-transform infrared spectroscopy
IC	inorganic content
MC	moisture content
MCE	modified combustion efficiency
MLR	mass loss rate
m	mass measured
Δm	mass loss
$\dot{m}$	mass loss rate of the peat sample
$\dot{m}''$	mass flux (mass flow rate per unit surface area)
PM	particulate matter
t	time
$\dot{V}$	volumetric flow rate
φ_ω	moisture content of the peat in dry base
ρ	density
$[i]$	concentration of a gas species i
Δt	measurement time interval
Δi	excess mixing ratio of a gas species i

Subscripts

d	dry peat base
i	gas species i
j	particle species j
w	wet peat base
b	calculated from carbon balance assumption
m	calculated from mass loss rate

gaseous pyrolysate releases the heat; in smouldering, heterogeneous oxidation occurs on the surface of the solid fuel, mostly char [3]. Each location of burning peat sees the successive arrival of four distinct thermal and chemical waves (sub-fronts) that form the structure of a smouldering front: preheating, evaporation, pyrolysis and oxidation [4,5]. In preheating and evaporation fronts (temperature below 100°C), only water vapour is emitted in large quantities and is not involved in chemical reactions. Char is formed in the pyrolysis front (temperature above 200°C and in the absence of oxygen), emitting volatile organic species (e.g., CH_4), trace levels of CO_2 and CO, and water vapour. Substantial CO_2 and CO are released in the exothermic char oxidation front (usually over 350°C) [4,5]. In open combustion conditions, the fire has natural oxygen supply, thus the pyrolysis front overlaps with the oxidation front.

Smouldering peat fires generate weakly buoyant smoke plumes that accumulate close to the ground. Driven by wind, the emissions can migrate long distances, causing regional air quality deterioration (haze phenomena), transportation disruption and vast economic losses [6]. These emissions are complex mixtures of incomplete combustion gases (up to ~90 detectable gas species) and aerosols containing substantial quantities of particulate matter (PM) which ranges from ultrafine particles (aerodynamic diameter $\leq 0.1 \, \mu m$) to PM_1 ($\leq 1 \, \mu m$), $PM_{2.5}$ ($\leq 2.5 \, \mu m$) and PM_{10} ($\leq 10 \, \mu m$) [7]. Exposure of large population, like those in Southeast Asia, to haze can induce millions of respiratory and cardiovascular health emergencies [6].

Smouldering peat fires propagate horizontally and vertically through deep layers (up to more than 1 m in depth) for weeks or months, leading to the largest fires on Earth, in terms of the mass of fuel consumed per unit surface [2]. Carbon emissions from peat fires play an important role in global climate change and the carbon budget balance. For example, between 0.81 and 2.57 Gt of carbon were released during the 1997 Southeast Asia extreme peat fire event, equivalent to 13–40% of the mean annual global carbon emissions from fossil fuels of that year [8]. The release of ancient (up to 10,000 years old) carbon stored in peat creates a positive feedback to the climate system, a self-accelerating process [2].

Among all the parameters used to quantify fire emissions, the emission factor (*EF*), defined as the mass of species emitted per mass of dry fuel consumed, is especially useful when combined with remote sensing technologies like satellites for atmospheric chemistry modelling and for carbon budget calculations [9]. Most of the peat fire EF has been measured by airborne and field measurements [7,9]. However, large EF variability exist in literature, uncertainties remain in both EF quantification and the determination of the combustion regimes [6]. This variability is not understood, and how the emissions correlate with combustion dynamics are not part of previous studies, except for two studies where this is done for only CO_2 and CO [4,10].

In this work, the transient mass flow rate and EF of up to 20 different gas species, and size-fractioned particles from smouldering combustion of peat were simultaneously measured under controlled laboratory conditions for the first time. The relationships between the emissions and the combustion dynamics were also examined.

2. Experimental method

A commercially available temperate Irish sphagnum peat (Shamrock Irish Moss Peat, Bord na Mona Horticulture Ltd.) was used in the experiments. This peat has homogeneous properties and composition and has been used in previous work [11]. Elemental analysis (dry basis) shows that the mass fraction of C/H/N/S of this peat is 54.1/5.1/1.3/0.5%, respectively. Peat moisture content (*MC*), defined as the mass of water divided by the mass of a dried peat sample (expressed as %), varies from 10% under drought conditions to > 300% in flooded scenarios [11,12]. Following
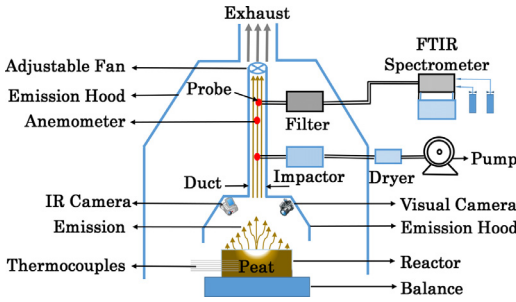
Fig. 1. Schematic of the smouldering peat emission experiment set-up. The rig is comprised of four main parts: smouldering reactor, emission collector, residual gas treatment system and diagnostics for measuring dynamics and emissions.

the drying and rewetting protocol developed in [4,11], a MC of 100%, representative of natural unperturbed conditions, was targeted. The actual MC obtained is $103 \pm 1.1\%$. The measured bulk density and the inorganic content (*IC*) of the wet peat sample are $243 \, \mathrm{kg \, m^{-3}} \pm 2\%$ and $2.5 \pm 1\%$, respectively.

An open-top reactor with internal dimensions of $20 \times 20 \times 10$ cm, built from 1.3 cm thick mineral wool board, was used for the burning of the peat samples under controlled conditions, as used in previous work [11,13]. An 18 cm coil heater is mounted on one side of the reactor, 5 cm below the free surface. The sample was ignited by applying 100 W of power to the coil for 30 min. This ignition protocol is strong enough to initiate a self-sustained smouldering with peat MC < 150% [13]. The emissions were collected using an inverted fume extraction hood located at a certain skirt free height (the distance between the hood and the reactor), and were transported into a duct, where a fan controls the extraction rate (Fig. 1). The fan speed was manually set to avoid smoke escaping from the hood, the environmental temperature and humidity were constantly monitored.

Six different diagnostics were used: mass loss (Mettler Toledo balance, resolution 0.01 g), temperature profile (twelve K-type thermocouples (TCs) array, 3 rows × 4 columns), visual and infrared (*IR*) imaging of the surface spread (Go-Pro and FLIR camera), transient gas (Thermo Scientific Nicolet iG50 Fourier-transform infrared spectroscopy (FTIR)) and PM (Dekati 4-stage PM cascade impactor). All ducts of the FTIR are constantly heated to 100 °C by a heat controller to avoid gas condensation. Based on the gas calibration and built-in least-squares algorithm of the FTIR, the real-time concentration of the 20 different gas species which are most commonly reported in the fire literature were measured: carbon dioxide (CO_2), carbon monoxide (CO), methane (CH_4), acetylene (C_2H_2), ethylene (C_2H_4), ethane (C_2H_6), propylene (C_3H_6), propane (C_3H_8),

butane (C_4H_{10}), methanol (CH_3OH), formaldehyde (CH_2O), nitric oxide (NO as NO_x), nitrogen dioxide (NO_2), hydrogen cyanide (HCN), acetic acid (CH_3COOH), acetaldehyde (C_2H_4O), formic acid (CH_2O_2), hydrogen chloride (HCl), ammonia (NH_3) and sulphur dioxide (SO_2).

Size-fractioned particles ($D \geq 10 \, \mu m$; $2.5 \, \mu m \leq D \leq 10 \, \mu m$; $1 \, \mu m \leq D \leq 2.5 \, \mu m$; $D \leq 1 \, \mu m$) were sampled in accordance with ISO 23210 using an isokinetic probe, and were collected onto 4 different aluminium filters inside each of the stages of the impactor. The post-sampling particles from each stage (for 15 min every 2 h) were weighed immediately using a Sartorius balance (resolution 0.01 mg). The PM_{10}, $PM_{2.5}$ and PM_1 are calculated by the mass gain of each filter from the relevant impactor stages.

Preliminary experiments were conducted to characterise the experimental rig (Fig. 1). By varying the forced ventilation (measured as the duct mid-point velocity) and the skirt free height in each experiment, a $2 \, \mathrm{m \, s^{-1}}$ duct velocity with 2 cm skirt free height was found to collect all the smoke from the reactor, and have the same mass loss rate (*MLR*) and surface spread rate as open conditions. The mass flow rate profile across the duct diameter was found to be within $\pm 10\%$ of the averaged value, which means the flow is well mixed. Each experiment was repeated 5 times (ambient temperature 20.4 ± 0.8°C, relative humidity $45.8 \pm 7.6\%$). Each experiment was terminated about 10.5 h from ignition, at which time the fire was gradually extinguishing and near burn out, because it has reached the far walls of the reactor.

3. Results and discussion

3.1. Combustion dynamics, transient gas species and PM

Figure 2 shows MLR vs. real-time [CO_2], [CO] and PM for one of the experiments. All experiments had similar time evolution to these variables. Examining the MLR measurements, four different combustion stages were observed (ignition, growth, steady and burn out): During the ignition stage the MLR rapidly increased, peaking at $0.028 \, \mathrm{g \, s^{-1}}$ (I, 0–30 min). A steady increase in MLR was observed in the growth stage when the burning area increased (II, 30–225 min), followed by the steady stage where the MLR stayed between 0.025–$0.030 \, \mathrm{g \, s^{-1}}$ (III, 225–450 min). The MLR decreased between 0.010–$0.025 \, \mathrm{g \, s^{-1}}$ in the burn out stage (IV, 450–630 min). The variations in the MLR throughout the experiments can be explained by the combustion dynamics involved in each stage.

In the ignition stage, the heat from the ignition coil generates a pyrolysis forming char and releasing gases of the thermal decomposition, resulting in an increased MLR [4,5]. The porous peat
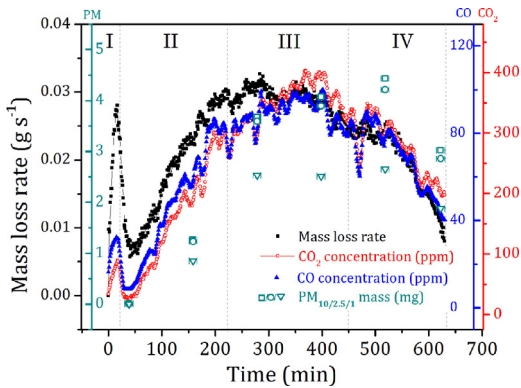
Fig. 2. Example evolution of MLR, [CO$_2$], [CO] (curves smoothed) and PM measured during a 100% MC smouldering peat experiment. Vertical dashed lines indicate each stage of the fire combustion regimes: (I) ignition stage; (II) growth stage; (III) steady stage and (IV) burn out stage.
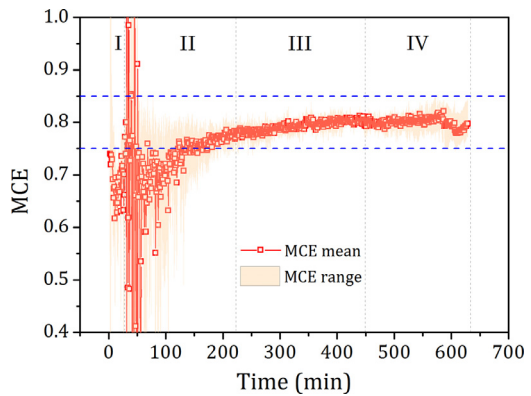

Fig. 3. MCE evolution for smouldering peat experiments. Vertical dashed lines indicate each stage of the fire combustion regimes. Horizontal dashed lines indicate the smouldering thresholds (0.75–0.84) as proposed by [7].

facilitates the heterogeneous reaction with oxygen and permits the transport of oxygen through the fuel bed [3]. The heat released from the exothermic char oxidation is transferred to the adjacent peat, spreading the smouldering front. The increasing width of the smouldering front across the surface of the peat bed causes a nearly linear increase of MLR with time during the growth stage.

According to the visual and IR imaging observations, the surface area of the burning peat stayed relatively constant throughout the steady stage (Fig. S1). Temperature profile shows that within the steady stage, peat temperature peaked (around 600°C) in the bottom layer (8 cm below the free surface), while the middle (5 cm below) and the top layer (2 cm below) stayed below 250°C and 120°C, respectively. Tracking the temperature profile by using the drying front (100°C) as a marker [11], the lateral spread rates (leading edge) of the upper, middle and bottom layers are 1.9 ± 0.3 cm h^{-1}, 1.4 ± 0.3 cm h^{-1} and 2.3 ± 0.4 cm h^{-1}, respectively (Fig. S2). This spread rate difference with depth leads to the formation of an overhang [11]. The periodic collapse of the overhang results in the fluctuation of MLR observed during the experiments (Fig. 2). The decrease of the MLR during the burn-out stage is caused by the arrival of the leading edge to the far wall [4].

Regarding the transient gas species, both the [CO$_2$] and [CO] followed the MLR trend closely. Intensified pyrolysis emits trace levels of CO$_2$ and CO, leading to the first concentration peak observed during the ignition stage [4,5]. The char oxidation is the main source of CO$_2$ and CO [4,14]. As a result, their concentrations peak at the steady stage, fluctuating at 350 ± 50 ppm and 90 ± 10 ppm, respectively. PM also followed a similar pattern to the MLR evolution. For example, the

PM$_1$ mass increased from 0.85 mg (growth stage) to 2.52 mg (steady stage) and decreased to 1.88 mg when the experiment was terminated (burn out stage).

The transient concentrations of the other gas species from all experiments are shown in Fig. S3. Not all gas species show a similar evolution to CO$_2$ and CO. Notably, CH$_4$, C$_2$H$_6$, C$_2$H$_4$, C$_3$H$_8$, C$_4$H$_{10}$ and C$_2$H$_4$O reach a maximum concentration during the ignition stage, indicating they are mainly emitted during pyrolysis [4,5]. Not included in the figure are CH$_3$COOH and HCl as their concentrations were below the detection limit throughout the experiments, possibly due to their negligible emissions from smouldering peat or the heavy interference with other volatile organic compounds.

In the remote sensing and atmospheric sciences literature, a modified combustion efficiency (*MCE*) is widely applied to classify the combustion regimes of biomass burning (Eq. (1)) [7,9,15,16].

$$MCE = \frac{\Delta CO_2}{\Delta CO + \Delta CO_2} \tag{1}$$

where Δ is the excess mixing ratio (the mole fraction of species in the smoke minus that from the background air).

An averaged MCE over the whole fire episode is commonly reported in the literature to represent the overall fire behaviour. It has been reported that the MCE of a smouldering fire ranges between the thresholds of 0.75 and 0.84 [7]. Figure 3 shows the MCE evolution throughout our laboratory experiments. There is a substantial variability of the MCE among the different combustion stages: it ranges from 0.68 ± 0.04 (ignition stage), to 0.62 ± 1.44 (growth stage), to 0.79 ± 0.01 (steady stage) and 0.80 ± 0.01 (burn out stage). MCE during the ignition and the growth stages is below the threshold. Moreover, there is no MCE difference between the steady and burn-out stage. These MCE

variations contradict the combustion dynamics driving the MLR changes. This failure of the MCE to explain smouldering fires is due to the fact that peat fire is a complex combustion phenomenon. This conclusion was also recently reached in a related work where we looked at MCE values reported in the literature for smouldering fires [6].

3.2. Transient PM species EF

The EF of PM species j (PM_{10} or $PM_{2.5}$ or PM_1) as a function of time is determined by using Eq. (2).

$$EF_j(t) = \frac{m_j(t)}{\Delta m_d(t)} \frac{\dot{V}}{\dot{V}_j} \tag{2}$$

where $m_j(t)$ is the time-resolved mass of sampled PM; $\Delta m_d(t)$ is the mass loss of dry peat; $\dot{V}$ is the volumetric flow rate within the duct (0.035 $m^3s^{-1} \pm 2.5\%$) and $\dot{V}_j$ is the PM sampling flow rate within the impactor (0.0005 $m^3s^{-1} \pm 5.0\%$, leading to a $\pm 2.8\%$ accuracy in the size of particles collected with 50% efficiency on each particular impactor stage). Because the measurement of water vapour is challenging with the FTIR (sensitivity to ambient relative humidity and cleaning protocol), $\Delta m_d(t)$ is calculated instead by assuming that drying is constant, and the fraction of the rate of the moisture emission corresponds to the MC of the peat, according to (Eq. (3)) [4].

$$\Delta m_d(t) = \frac{m_{w(t+\Delta t)} - m_{w(t)}}{(1 + \varphi_\omega)} \tag{3}$$

where $m_{w(t+\Delta t)}$ and $m_{w(t)}$ are the mass of the wet peat before and after each PM measurement interval; Δt is the single measurement time (15 min); φ_ω is the MC of the peat sample in dry basis.

Reports of PM EF and their emission mechanism from smouldering peat fires are scarce [6]. This work provides the first comprehensive size-fractioned PM EF transient data for smouldering peat fires (Fig. 4). Combined with the uncertainty of the extraction rate, the total uncertainties in the measurements of PM_1, $PM_{2.5}$ and PM_{10} EF are $\pm 16.4\%$, $\pm 19.2\%$ and $\pm 22.0\%$, respectively. Here we report the average EF from the steady stage, as it is the most representative of free fire propagation, and least affected by edges and scale effects [4]: PM_{10} (24.48 ± 1.06 g kg^{-1}), $PM_{2.5}$ (23.12 ± 1.19 g kg^{-1}) and PM_1 (15.04 ± 1.12 g kg^{-1}). The $PM_{2.5}$ EF found in these experiments is close to 19.17 ± 6.8 g kg^{-1} reported in [6]. The mass fraction of different-sized particles remain relatively constant throughout the experiments: PM_{10} occupies $99.4 \pm 0.7\%$ of all the detectable particles, while $PM_{2.5}$ and PM_1 take up $87.2 \pm 18.6\%$ and $58.4 \pm 13.7\%$ of the total particle mass.
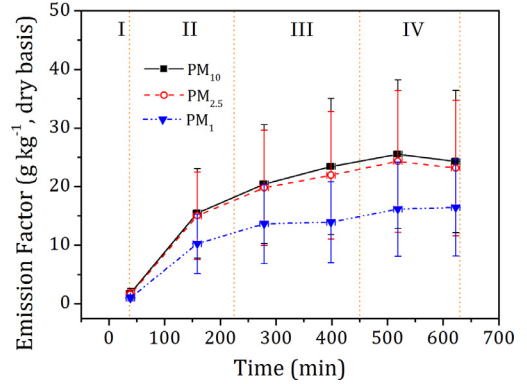

Fig. 4. EF evolution PM_{10}, $PM_{2.5}$ and PM_1 from the 100% MC smouldering peat experiments. Vertical dashed lines mark the end of each combustion regime.

3.3. Transient gas species EF

Rein et al. [4] and Hadden [10] reported the average CO_2 and CO mass flow rates per area of smouldering front (mass flux). In this work, the transient mass flux of all 20 gas species ($\dot{m}''_{g,i}(t)$) is calculated using Eq. (4) and is showed in Fig. S4.

$$\dot{m}''_{g,i}(t) = \rho_i[i](t)\dot{V} \tag{4}$$

Where ρ_i is the species density (ideal gas assumption); $[i](t)$ is the real-time concentration of the species i. Species' background concentration were measured and subtracted from the results.

Averaging the steady stage, the mass flux for CO_2 is $\dot{m}''_{g,CO_2} = 0.60 \pm 0.07$ g s^{-1} m^{-2}, which is very close to 0.65 ± 0.24 g s^{-1} m^{-2} reported in [4]. For CO, this work reports a 3 times lower, $\dot{m}''_{g,CO} = 0.09 \pm 0.007$ g s^{-1} m^{-2}, than 0.27 ± 0.09 g s^{-1} m^{-2} [4]. CH_4 and NH_3 present the two largest mass fluxes among the other trace gas species, reaching 0.0046 ± 0.0005 and 0.0045 ± 0.0006 g s^{-1} m^{-2}, respectively.

The transient EF for gas species i ($EF_{m,i}(t)$, g kg^{-1}) using Eq. (5), is the same to the species yield (γ_i, % g g^{-1}) used in combustion, like [4]:

$$EF_{m,i}(t) = \frac{\dot{m}''_{g,i}(t)}{\left(\frac{\dot{m}_w(t)}{1+\varphi_\omega}\right)} \tag{5}$$

Where $\dot{m}_w(t)$ is the time-resolved MLR of the wet peat sample. The calculation of the dry peat MLR is also based on the constant moisture emission fraction assumption in Eq. (3) [4]. Factoring the uncertainty of all variables (MLR has an estimated uncertainty of $\pm 5\%$, while the gas concentration has a calibrated FTIR average uncertainty of $\pm 10\%$), the estimated total uncertainty of any gas species EF_m is $\pm 18.6\%$.

Instead of the real-time EF used in this work, a carbon balance approach is widely used in remote
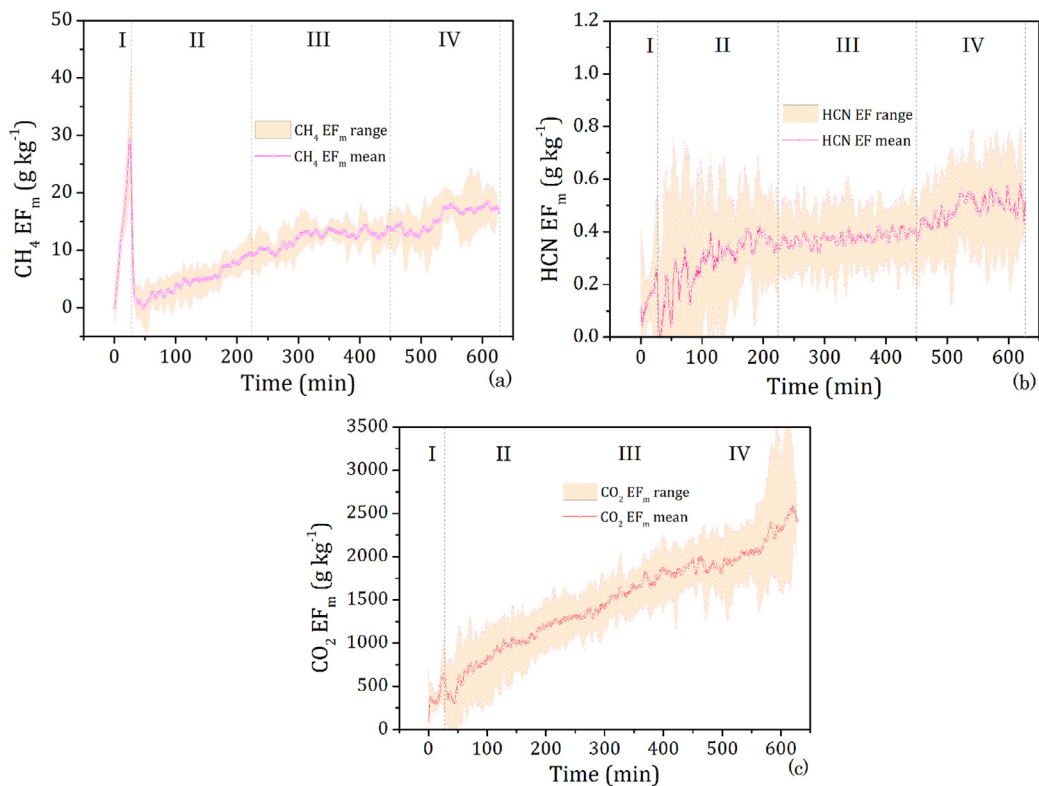
Fig. 5. EF_m evolution of (a) CH_4 (group A species); (b) HCN (group B species); (c) CO_2 (group C species). An EF mean and range from all the 5 repeated 100% MC smouldering peat experiments are shown. Vertical dashed lines indicate each of the fire regimes.

sensing and atmospheric sciences in the literature to calculate the EF for gas species i ($EF_{b,i}$, g kg^{-1}) without obtaining the MLR (Eq. 6). This approach assumes all of major carbon-containing emissions have been measured [7,15,16].

$$EF_{b,i} = F_c \cdot 1000 \ (\text{g kg}^{-1}) \cdot \frac{MM_i}{12} \cdot \frac{C_i}{C_T} \qquad (6)$$

Where F_c is the peat carbon content (%, on dry mass basis), MM_i is the molar mass of species i, C_i is the number of moles of species i, and C_T is the total number of moles of carbon emitted.

Compared with the extensive number of publication reporting EF_b values, studies investigating EF_m remain scarce [4,10]. This is because MLR is often difficult to obtain, and impossible for field measurements [7]. In this work, the transient EF_m of multiple gas species are calculated for the first time. Based on the evolution characteristics of the EF_m, the 20 gas species are classified into four groups: (A) EF_m peaks within the ignition stage for CH_4, C_2H_6, C_3H_8 and C_4H_{10}; (B) EF_m stays flat in the steady stage for C_2H_2, C_2H_4, C_3H_6, CH_2O, CH_2O_2, C_2H_4O, CH_3OH, HCN, NO, NO_2, and SO_2; (C) EF_m increases steadily in the steady stage

for CO_2, CO and NH_3; (D) EF_m stays < 0.01 g kg^{-1} in the steady stage for CH_3COOH and HCl.

Figure 5 shows the EF_m evolutions of CH_4 (a), HCN (b) and CO_2 (c) as examples of the trends exhibited by group A, B and C, as all species within each group behaved similarly (EF_m evolutions of all the species in the four groups are summarised in Fig. S5–8). Group A species are all alkanes. Hydrocarbons like CH_4 are found to be mainly emitted from the decomposition of hemicellulose and cellulose in peat pyrolysis [4,5,17], leading to their EF_m peaking at the ignition stage. Averaging the steady stage, the CH_4 and C_4H_{10} EF are higher than the values reported in [6,7], while C_2H_6 and C_3H_8 EF are around 3 times smaller than found in literature (Table. S1).

Values of EF_m in Group B stay relatively constant within the steady stage. C_2H_4 and CH_3OH emissions have been observed from the pyrolysis [5,17]. Among the species in Group B, our EF_m measurements for HCN are on the low end of the literature range [6]. In contrast, the EF_m values of C_2H_2, C_2H_4, CH_2O, C_2H_4O are on the high end, especially for C_2H_4 and C_2H_4O, whose EF_m are around 5 times higher than in [7]. The EF_m of SO_2
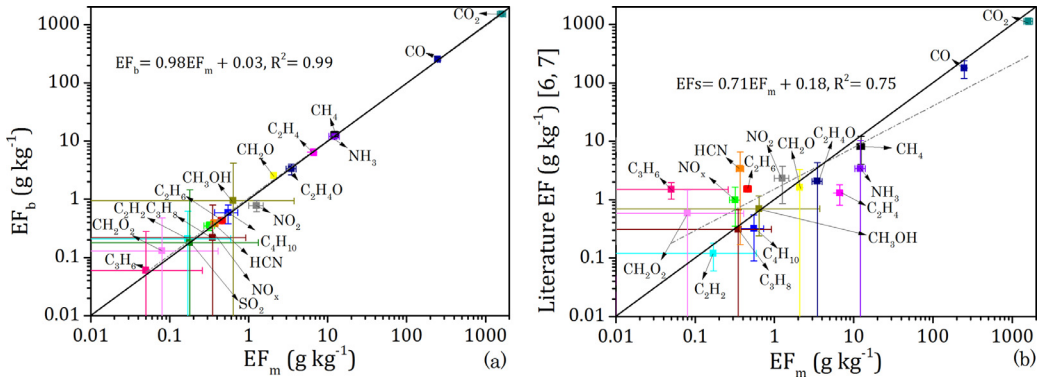
Fig. 6. Comparison of EF using mass loss rate (EF_m) with (a) EF calculated from the carbon balance approach (EF_b); (b) peat fire EF reported in literature [6,7].

$(0.18 \pm 1.15 \, \text{g kg}^{-1})$ are reported for the first time and are likely resulting from the oxidation of the sulphur in the peat sample (Table. S1).

For group C species, the increasing EF_m are probably because of char oxidation [4]. The increase also indicates that the proportion of the char being oxidised increases throughout this stage, leading to an average EF_m of CO_2 $(1,606 \pm 201 \, \text{g kg}^{-1})$ and CO $(248 \pm 15.8 \, \text{g kg}^{-1})$ (Table. S1). The ongoing increases of EF_m in the burn out stage are mainly attributed to the rapid decrease of the MLR. Peat fire NH_3 EF_m from in this work $(12.18 \pm 1.86 \, \text{g kg}^{-1})$ is 20 times larger than those found in flaming savannah fires [6,9]. Because of these findings, NH_3 could be a candidate atmospheric marker for smouldering peat fires in the field.

The steady-stage-average EF_m and EF_b calculating from Eqs. (5) and (6), together with the literature peat fire EF are summarised in Table. S1. This allows a direct comparison between the two EF methods: EF_b and EF_m are generally similar, however EF_b is on average $\sim6\%$ higher than EF_m. This is mainly because EF_b relies on the carbon balance assumption which fails to take into account the carbon from the unidentified high molecular species and the PM emissions (e.g., $23.12 \, \text{g kg}^{-1}$ $PM_{2.5}$ from this work), leading to a slight inflation of EF_b values. However, EF_m correlates well with EF_b ($R^2 = 0.99$) (Fig. 6a), which helps to validate the method for EF_b, which had not been validated before.

EF_m correlates well ($R^2 = 0.75$) with EF values found in the literature (also calculated based on carbon balance [6,7]) (Fig. 6b). This helps verify the transient EF_m calculation method used in this work. The difference between EF_m and the literature EF may stem from the different peat used in each study (e.g., temperate Irish peat in this work vs. tropical Kalimantan peat in [7]), as the peat sample composition is shown to affect the emissions [6]. Furthermore, all the results presented in this work are for samples at 100% MC. However, the emission behaviour and the combustion dynamics are expected to vary with different MC values [2,4], which will be investigated further in ongoing research.

4. Conclusion

Simultaneous measurements of mass loss, up to 20 gas species concentrations, particle mass (PM_{10}, $PM_{2.5}$ and PM_1), temperature profiles, surface visual and infrared imaging from the smouldering combustion of 100% moisture content peat have been conducted under controlled laboratory environment. This novel framework enables, for the first time, the correlation of the transient emissions to the combustion dynamics of smouldering peat fires.

The transient gas and particle emissions are shown to be significantly dependent on the combustion dynamics which helps explain the transient concentration and mass loss rate evolutions among four combustion stages (ignition, growth, steady and burn out). The modified combustion efficiency, a fire behaviour proxy widely used in remote sensing and atmospheric sciences, has been found to be a poor description of the complex smouldering peat phenomenon as it fails to capture the changing combustion dynamics.

Smouldering peat was found to emit gas species with different fluxes, with CO_2 $(0.60 \, \text{g s}^{-1} \, \text{m}^{-2})$ and CO $(0.09 \, \text{g s}^{-1} \, \text{m}^{-2})$ dominating, followed by CH_4 $(0.0046 \, \text{g s}^{-1} \, \text{m}^{-2})$ and NH_3 $(0.0045 \, \text{g s}^{-1} \, \text{m}^{-2})$. Thanks to the measurement of the mass loss rate, this work provides the first transient emission factor (EF_m) of both particle and gas species. Averaging the steady stage, PM_{10}, $PM_{2.5}$ and PM_1 EF_m reached $24.48 \, \text{g kg}^{-1}$, $23.12 \, \text{g kg}^{-1}$ and $15.04 \, \text{g kg}^{-1}$, with $PM_{2.5}$ representing 87.2% of the total particle mass. All alkane species (CH_4, C_2H_6, C_3H_8 and

C_4H_{10}) EF_m were found to peak within the ignition stage, mainly due to the intensified pyrolysis; CO_2, CO and NH_3 EF_m increase steadily in the steady stage, indicating they are mainly emitted by char oxidation. Owing to the 20 times larger EF_m of NH_3 measured in this work (12.18 g kg^{-1}) than those found in flaming savannah from the literature, it is proposed as an atmospheric tracer for smouldering peat fires.

For the first time, the validation of the gas species EF calculated from the carbon balance approach (EF_b) has been conducted here. The combustion dynamics are proven to explain in fundamental terms of the transient emissions from smouldering fires. This work contributes to the understanding of peat fire emissions and helps develop strategies tackling regional haze.

Supplementary materials

Supplementary material associated with this article can be found, in the online version, at doi:10.1016/j.proci.2018.06.008.

References

[1] M.R. Turetsky, B. Benscoter, S. Page, et al., *Nat. Geosci.* 8 (2015) 11–14.
[2] G. Rein, Fire Phenomena and the Earth System, Wiley and Sons, 2013, pp. 15–33.
[3] G. Rein, et al., SFPE Handbook of Fire Protection Engineering, Springer, 2015, pp. 581–603.
[4] G. Rein, S. Cohen, A. Simeoni, *Proc. Combust. Inst.* 32 (2009) 2489–2496.
[5] A. Usup, Y. Hashimoto, H. Takahashi, H. Hayasaka, *Tropics* (2004) 14.
[6] Y. Hu, N Fernandez-Anez, T.E.L. Smith, G. Rein, *Int. J. Wildland Fire* 27 (2018) 293–312.
[7] C.E. Stockwell, T. Jayarathne, M.A. Cochrane, et al., *Atmos. Chem. Phys.* 16 (2016) 11711–11732.
[8] S.E. Page, F. Siegert, J.O. Rieley, H.-D.V. Boehm, A. Jaya, S. Limin, *Nature* 420 (2002) 61–65.
[9] S.K. Akagi, et al., *Atmos. Chem. Phys.* 11 (2011) 4039–4072.
[10] R. Hadden, Smouldering and Self-Sustaining Reactions in Solids: An Experimental Approach, Ph.D. thesis, The University of Edinburgh, Edinburgh, UK, 2011.
[11] X. Huang, F. Restuccia, M. Gramola, G. Rein, *Combust. Flame* 168 (2016) 393–402.
[12] X. Huang, G. Rein, H. Chen, *Proc. Combust. Inst.* 35 (2015) 2673–2681.
[13] G. Rein, N. Cleaver, C. Ashton, P. Pironi, J.L. Torero, *Catena* 74 (2008) 304–309.
[14] X. Huang, G. Rein, *Bioresour. Technol.* 207 (2016) 409–421.
[15] D. Wilson, S.D. Dixon, R.R. Artz, et al., *Biogeosciences* 12 (2015) 5291–5308.
[16] C. Paton-Walsh, T.E. Smith, E.L. Young, D.W. Griffith, É.A. Guérette, *Atmos. Chem. Phys.* 14 (2014) 11313–11333.
[17] L.E. Holst, L.A. Andersson, I. Bjerle, *Fuel* 70 (1991) 1017–1022.